

# Vibrational dephasing mechanisms in liquids and glasses: Vibrational echo experiments

K. D. Rector and M. D. Fayer

*Department of Chemistry, Stanford University, Stanford, California 94305*

(Received 16 September 1997; accepted 27 October 1997)

Picosecond vibrational echo studies of the asymmetric stretching mode ( $2010\text{ cm}^{-1}$ ) of (acetylacetonato)dicarbonylrhodium(I) [ $\text{Rh}(\text{CO})_2\text{acac}$ ] in liquid and glassy dibutyl phthalate (DBP) (3.5 K to 250 K) are reported and compared to previous measurements of a similar mode of tungsten hexacarbonyl [ $\text{W}(\text{CO})_6$ ]. The  $\text{Rh}(\text{CO})_2\text{acac}$  pure dephasing shows a  $T^1$  dependence on temperature at very low temperature with a change to an exponentially activated process ( $\Delta E \cong 400\text{ cm}^{-1}$ ) above  $\sim 20$  K. There is no change in the functional form of the temperature dependence in passing from the glass to the liquid. It is proposed that the  $T^1$  dependence arises from coupling of the vibration to the glass's tunneling two level systems. The activated process arises from coupling of the high-frequency CO stretch to the  $405\text{ cm}^{-1}$  Rh–C stretch. Excitation of the Rh–C stretch produces changes in the back donation of electron density from the rhodium  $d_\pi$  orbital to the CO  $\pi^*$  antibonding orbital, shifting the CO stretching transition frequency and causing dephasing. In contrast,  $\text{W}(\text{CO})_6$  displays a  $T^2$  dependence below  $T_g$  in DBP and two other solvents. Above  $T_g$ , there is a distinct change in the functional form of the temperature dependence. In 2-methylpentane, a Vogel–Tammann–Fulcher-type temperature dependence is observed above  $T_g$ . It is proposed that the triple degeneracy of the  $T_{1u}$  mode of  $\text{W}(\text{CO})_6$  is broken in the glassy and liquid solvents. The closely spaced levels that result give rise to unique dephasing mechanisms not available in the nondegenerate  $\text{Rh}(\text{CO})_2\text{acac}$  system. © 1998 American Institute of Physics. [S0021-9606(98)51705-9]

## I. INTRODUCTION

A molecule in a condensed matter medium, such as liquid or a glass, is influenced by intermolecular interactions with the surrounding solvent. The shift in vibrational frequencies in going from the gas phase to a condensed phase is an indication of the effect of the solvent on internal mechanical degrees of freedom. The static shift in vibrational absorption energies is a reflection of the average force exerted by solvent on the molecular oscillators. The medium also exerts fluctuating forces on the internal degrees of freedom of a solute molecule, which are responsible for fluctuations in molecular structure. The structural fluctuations are manifested in time-dependent vibrational eigenstates, and, thus, time-dependent vibrational energy eigenvalues. Fluctuating forces are involved in a wide variety of chemical and physical phenomena, including thermal chemical reactions, promotion of a molecule to a transition state, electron transfer, and energy flow into and out of molecular vibrations.

The dynamics of the bath of modes, which cause time evolution of the vibrational energy eigenvalues, give rise to fluctuations in vibrational energy level separations. The bath contains bulk solvent degrees of freedom arising from translational and orientation motions of the solvent molecules as well as the internal vibrational degrees of freedom of the solvent. The bath also contains the solute's vibrational modes other than the oscillator of interest. In a glass, bath frequency fluctuations range from very high frequency to essentially static. For a pair of energy levels, e.g.,  $v=0$  and  $v=1$ , the very fast fluctuations produce homogeneous pure dephasing, which, for an exponential decay of the off-

diagonal density matrix elements (Lorentzian homogeneous line shape), can be characterized by an ensemble average pure dephasing time,  $T_2$ . The total homogeneous dephasing time,  $T_2$ , also has contributions from the vibrational lifetime,  $T_1$ . Evolution of the system on time scales substantially slower than  $T_2$  appear as inhomogeneous broadening. In a glass, the time scale of the slowest system evolution may be so long that there is essentially truly static inhomogeneous broadening. However, there are also slow fluctuations that do not contribute to homogeneous pure dephasing but give rise to spectral diffusion. Spectral diffusion has been observed frequently in electronic excitation dephasing experiments in glasses,<sup>1–3</sup> and has also been observed for vibrational transitions.<sup>4,5</sup>

Identical considerations apply to homogeneous dephasing in liquids. There is a range of high-frequency fluctuations that give rise to homogeneous pure dephasing. Compared to this time scale, there can be inhomogeneous broadening arising from more slowly evolving components of the liquid structure. However, unlike a glass, there are no essentially static local environments that give rise to permanent inhomogeneous broadening. In a liquid, spectral diffusion will cause all possible transition energies to be sampled by an oscillator on some time scale.

In principle, information on dynamical intermolecular interactions of an oscillator with its environment can be obtained from vibrational absorption spectra. The vibrational line shape, line width, and their dependences on temperature and the nature of the solvent depend on the forces experienced by the oscillator. However, a vibrational absorption

spectrum reflects the full range of broadening of the vibrational transition energies, both homogeneous and inhomogeneous. In glasses and in liquids, inhomogeneous broadening can exceed the homogeneous line width. Under these circumstances, measurement of the absorption spectrum does not provide information on vibrational dynamics.

The ultrafast infrared (IR) vibrational echo experiment eliminates inhomogeneous broadening and provides a direct measurement of homogeneous dephasing (homogeneous spectrum). The vibrational echo is the equivalent of the magnetic resonance spin echo developed in 1950<sup>6</sup> and the electronic excitation photon echo developed in 1964.<sup>7,8</sup> Using vibrational echoes to measure the homogeneous dephasing time ( $T_2$ ) and IR pump-probe experiments to measure the vibrational lifetime ( $T_1$ ) (and orientational relaxation if it occurs), the homogeneous pure dephasing time ( $T_2$ ) can be obtained.<sup>9–11</sup> Pure dephasing describes the adiabatic modulation of the vibrational energy levels of a transition caused by thermal fluctuations of its environment.<sup>12,13</sup> Measurement of this quantity provides detailed insight into the fast dynamics of the system. Thus, working in the time domain using nonlinear vibrational experiments, it is possible to determine the homogeneous spectrum and all dynamical contributions to it.

In this paper, detailed vibrational echo studies of (acetylacetonato)dicarbonylrhodium(I) [Rh(CO)<sub>2</sub>acac] in dibutyl phthalate (DBP) above and below the solvents glass transition temperature ( $T_g = 169$  K) are presented and compared to prior results for W(CO)<sub>6</sub> in several solvents including DBP.<sup>14</sup> In both metal carbonyls, the asymmetric CO stretching mode at  $\sim 2000$  cm<sup>-1</sup> is examined over a wide range of temperatures, temperatures at which the solvent is a low-temperature glass, passes through the glass transition, and is a liquid well above  $T_g$ . Of particular interest is the pure dephasing time,  $T_2^*$ , which reflects the medium induced transition energy fluctuations of the CO oscillator.

The CO asymmetric stretching modes of Rh(CO)<sub>2</sub>acac and W(CO)<sub>6</sub> are different in a manner that appears to be important. The Rh(CO)<sub>2</sub>acac mode ( $A_1$  of molecular point group  $C_{2v}$ ) is nondegenerate while the W(CO)<sub>6</sub> mode ( $T_{1u}$  of molecular point group  $O_h$ ) is formally triply degenerate in the gas phase. In a condensed phase, the local solvent structure will be anisotropic. In general, there will be different solute/solvent interactions along the molecular  $x$ ,  $y$ , and  $z$  axes. These anisotropic interactions will break the triple degeneracy of the  $T_{1u}$  mode of W(CO)<sub>6</sub>, yielding three modes with small energy splittings.

The results presented below show that Rh(CO)<sub>2</sub>acac has temperature-dependent pure dephasing with a different functional form than W(CO)<sub>6</sub> even when the solvent, DBP, is the same. At low temperature, in glassy DBP, the Rh(CO)<sub>2</sub>acac pure dephasing temperature dependence is linear,  $T^1$ , and is exponentially activated at higher temperatures.<sup>14</sup> In contrast, W(CO)<sub>6</sub> has a  $T^2$  temperature dependence in three different glassy solvents up to their corresponding  $T_g$ 's.<sup>9</sup> Above  $T_g$  in all three solvents, there is a change in the form of the temperature dependence. In 2-methylpentane (2MP), W(CO)<sub>6</sub> pure dephasing makes an abrupt transition from  $T^2$  to a Vogel–Tammann–Fulcher (VTF) type temperature

dependence.<sup>9</sup> Mechanisms are proposed to explain the temperature-dependent pure dephasing of Rh(CO)<sub>2</sub>acac, and differences between it and W(CO)<sub>6</sub> including the role of the different degeneracies of the modes of interest.

## II. THE VIBRATIONAL ECHO METHOD AND EXPERIMENTAL PROCEDURES

### A. The vibrational echo method

The vibrational echo experiment is a time domain third-order nonlinear experiment that can extract the homogeneous vibrational line shape even when the inhomogeneous line width is thousands of times wider than the homogeneous width.<sup>9,10,15</sup>

A source of ps IR pulses is tuned to the vibrational transition of interest to provide the vibrational echo two pulse excitation sequence. The first pulse excites each solute molecule into a superposition state, which is a mixture of the  $v = 0$  and  $v = 1$  vibrational states. Each superposition has a microscopic electric dipole associated with it. This dipole oscillates at the vibrational transition frequency. Immediately after the first pulse, all of the microscopic dipoles in the sample oscillate in phase. Because there is an inhomogeneous distribution of vibrational transition frequencies, the dipoles oscillate with some distribution of frequencies. Thus, the initial phase relationship is very rapidly lost. This effect is the free induction decay. After a time,  $\tau$ , a second pulse, traveling along a path making an angle,  $\theta$ , with that of the first pulse, passes through the sample. This second pulse changes the phase factors of each vibrational superposition state in a manner that initiates a rephasing process. At time  $2\tau$ , the ensemble of superposition states is rephased. The phased array of microscopic dipoles behaves as a macroscopic oscillating dipole which generates an additional IR pulse of light called the vibrational echo. The vibrational echo pulse propagates along a path that makes an angle,  $2\theta$ , with that of the first pulse. Subsequently, a free induction decay again destroys the phase relationships, so only a temporally short pulse of IR light is generated.

The rephasing at  $2\tau$  has removed the effects of the inhomogeneous broadening.<sup>16</sup> However, fast fluctuations due to coupling of the vibrational mode of interest to the bath cause the oscillation frequencies to fluctuate. Thus, at  $2\tau$  there is not perfect rephasing. As  $\tau$  is increased, the fluctuations produce increasingly large accumulated phase errors among the microscopic dipoles, and the signal amplitude of the vibrational echo is reduced. A measurement of the vibrational echo intensity versus  $\tau$  is an echo decay curve. Thus, the vibrational echo decay is related to the fluctuations in the vibrational frequencies, not the inhomogeneous spread in frequencies. The Fourier transform of the echo decay is the homogeneous line shape.<sup>16,17</sup> The vibrational echo makes the vibrational homogeneous line shape an experimental observable.

In the experiments on Rh(CO)<sub>2</sub>acac in DBP, orientational relaxation does not occur on the time scale of the vibrational echo experiments because of the high viscosity of the solvent at all temperatures studied. This fact was verified

experimentally using polarization selective pump-probe experiments. Therefore, orientational relaxation does not contribute to  $\text{Rh}(\text{CO})_2\text{acac}$  homogeneous dephasing. The role of orientational relaxation in vibrational echo experiments of  $\text{W}(\text{CO})_6$  has been previously discussed<sup>5</sup> and reanalyzed below.

The IR absorption line shape is related to these microscopic dynamics through the Fourier transform of the two-time transition dipole correlation function<sup>10,13,18–20</sup> which depends upon variations in the transition energies for the ensemble of vibrational transition dipoles and includes inhomogeneous broadening.<sup>3</sup> In the Markovian limit, and in the absence of inhomogeneous broadening, the transition dipole correlation function decays exponentially at a rate of  $1/T_2$ , where  $T_2$  is the homogeneous dephasing time. The Fourier transform gives a Lorentzian line shape, and contributions to the full line width at half maximum are additive

$$\Gamma = \frac{1}{\pi T_2} = \frac{1}{\pi T_2^*} + \frac{1}{2\pi T_1}. \quad (1)$$

Equation (1) allows the contribution of pure dephasing to the vibrational homogeneous line shape to be determined from a knowledge of the homogeneous line width and the vibrational lifetime.

The description of the third-order nonlinear polarization that governs vibrational echo experiments in terms of the dynamics of lifetime and pure dephasing has been presented.<sup>9</sup> For a Lorentzian homogeneous line, the vibrational echo signal pulses decays exponentially as

$$I(\tau)/I(0) = \exp[-4\tau(1/T_2^* + 1/2T_1)] \quad (2a)$$

$$= \exp[-4\tau/T_2]. \quad (2b)$$

The signal decays at a rate four times faster than the decay of the homogeneous dipole correlation function. If the pulse duration is comparable to  $T_2$ , a detailed calculation of the third-order polarization can be performed to extract  $T_2$ .<sup>21</sup>

## B. Experimental procedures

The vibrational echo experiments require tunable IR pulses with durations of  $\sim 1$  ps and energies of  $\sim 1 \mu\text{J}$ . The experiments described below were performed using IR pulses near  $\sim 5 \mu\text{m}$  generated by the Stanford superconducting-accelerator-pumped free electron laser (FEL).<sup>9</sup> The FEL generates nearly transform-limited pulses with a pulse duration that is adjustable between 0.7 and 2 ps. Active frequency stabilization allows wavelength drifts to be limited to  $<0.01\%$ , or  $<0.2 \text{ cm}^{-1}$ . The pulse duration, spectrum, and peak power are monitored continuously.

The FEL produces a 2 ms macropulse at a 10 Hz repetition rate. Each macropulse consists of the ps micropulses at a repetition rate of 11.8 MHz (84.7 ns). The micropulse energy at the input to experimental optics is  $\sim 0.5 \mu\text{J}$ .

To avoid sample heating problems, micropulses are selected out of each macropulse by Ge acousto-optic modula-

tor (AOM) single pulse selectors.<sup>9</sup> This pulse selection yields an effective experimental repetition rate of 1 kHz, and an average power  $<0.5 \text{ mW}$ .

The two pulses for the vibrational echo or the pump-probe (transient absorption to measure the vibrational lifetime) experiments were obtained using a 10% beamsplitter. The 10% beam (first pulse in vibrational echo sequence or probe pulse) is a single pulse selected using a Ge AOM and sent through a computer-controlled stepper motor delay line. The remaining portion (second echo pulse or pump pulse) is single pulse selected by a second Ge AOM. The AOMs can select pulses at either 25 or 50 kHz. For the vibrational echo experiment, the lower energy beam is selected at 25 kHz for background subtraction. For pump-probe, background subtraction is performed by selecting two adjacent micropulses. The two pulses were focused into the sample to  $\sim 50 \mu\text{m}$  diameter using an off-axis parabolic reflector. The signals are measured with HgMgTe detectors, gated integrators, and digitized for collection by computer.

Careful studies of power dependence and repetition rate dependence of the data were performed. It was determined that there were no heating or other unwanted effects when vibrational echo experiments were performed with pulse energies of  $\sim 15 \text{ nJ}$  for the first pulse and  $\sim 80 \text{ nJ}$  for the second pulse and the effective repetition rate of 1 kHz (50 kHz during each macropulse).

Vibrational echo and pump-probe data were taken on the  $A_1$  asymmetric CO stretching mode of  $\text{Rh}(\text{CO})_2\text{acac}$ . Solutions in DBP were made to give a peak optical density of 0.8 in a  $400 \mu\text{m}$  path length cell. These solutions correspond to mole fractions of  $\leq 10^{-4}$ . The temperatures of the samples were controlled to  $\pm 0.2 \text{ K}$  using a constant flow He cryostat.

The  $\text{Rh}(\text{CO})_2\text{acac}$  vibrational echo data had two forms due to its small vibrational anharmonicity ( $13.7 \text{ cm}^{-1}$ ).<sup>22,23</sup> For the short pulses used in these experiments, it is possible for the pulse bandwidth to exceed the anharmonic splitting. In this case, a three-level coherence is formed of the  $v=0, 1$ , and 2 levels. This produces a nonexponential vibrational echo decay with beats at the anharmonic splitting frequency.<sup>22,23</sup> When the laser wavelength is tuned to the center of the inhomogeneous line and the laser bandwidth is narrow, single exponential decays are measured. Further, single exponentials can be obtained with wider bandwidths by tuning the laser to the blue. In the decays with beats, the slowest component of the decay corresponds to the dephasing of the  $v=0-1$  transition only.<sup>22,23</sup> Both types of data were recorded and are reported here. Within experimental error, no differences in dephasing times were observed for the single exponential (narrow bandwidth) decays or the longest component of the nonexponential (wide bandwidth) decays. (The  $v=1-2$  dephasing time can be extracted from the fast component of the nonexponential decay.<sup>22,23</sup>)

## III. RESULTS

Vibrational echo experiments were conducted on the CO asymmetric stretching mode of  $\text{Rh}(\text{CO})_2\text{acac}$  ( $2010 \text{ cm}^{-1}$ ) in DBP from 3.4 K to 250 K. In addition, vibrational pump-

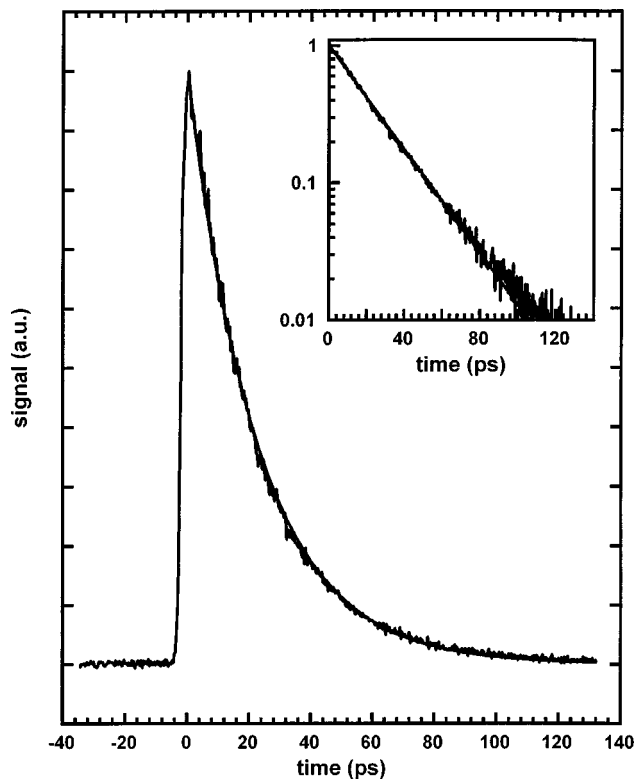


FIG. 1. Vibrational echo decay data of the asymmetric CO stretch mode of Rh(CO)<sub>2</sub>acac in DBP at 3.4 K. The decay is single exponential. The inset is a semilog plot of the data and fit. The decay constant is 23.8 ps, which yields a homogeneous line width of 0.11 cm<sup>-1</sup>. The absorption spectrum has a line width of ~15 cm<sup>-1</sup> at this temperature, demonstrating that the line is massively inhomogeneously broadened.

probe experiments were performed on the same transition from 3.4 K to 300 K. Figure 1 shows vibrational echo data taken at 2020 cm<sup>-1</sup> which is 10 cm<sup>-1</sup> to the blue of the center line at 3.4 K and a fit to an exponential decay [Eq. (2)]. The laser bandwidth for this data set is ~14 cm<sup>-1</sup>, so overlap with  $\nu = 1-2$  negligible. Within experimental uncertainty, the decay is a single exponential. Therefore, the homogeneous line shape is a Lorentzian. The decay constant  $T_2 = 95.2$  ps, yielding a homogeneous line width of 0.11 cm<sup>-1</sup>. For comparison, the absorption spectrum has a line width of ~15 cm<sup>-1</sup> at this temperature. The absorption line is massively inhomogeneously broadened. The vibrational echo experiments show that the absorption line is inhomogeneously broadened at all temperatures studied, including 250 K [ $1/(\pi T_2) = 1.5$  cm<sup>-1</sup>], which is ~80 K above  $T_g$ .

Figure 2 displays the results of the temperature-dependent vibrational echo (circles) and pump-probe (triangles, plotted as  $2T_1$ ) experiments. As with studies made on W(CO)<sub>6</sub> in a number of solvents, the temperature dependence of  $2T_1$  is very mild, and the temperature dependence of  $T_2$  is much steeper. Using Eq. (1) and the  $2T_1$  and  $T_2$  values obtained from the experiments, the pure dephasing,  $T_2^*$  can be obtained. There is a small amount of scatter in the pump-probe data. The scatter is insignificant at the higher temperatures where pure dephasing totally dominates the ho-

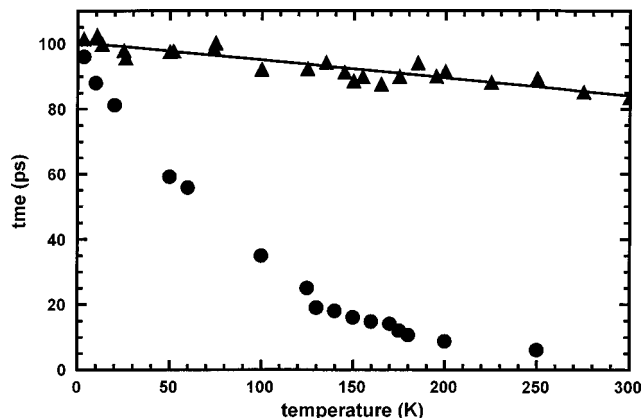


FIG. 2. Vibrational echo (circles) and pump-probe (triangles) data for the asymmetric CO stretch mode of Rh(CO)<sub>2</sub>acac in DBP. The pump-probe results are plotted as  $2T_1$ , in accordance with Eq. (1). The solid line through the  $T_1$  data is the best fit to the temperature dependence. Using these results, the temperature-dependent pure dephasing rates can be calculated from Eq. (1).

mogeneous line width. The solid line through the data is a fit to a straight line, which accurately reflects the temperature dependence of the  $T_1$  data over the full range of temperatures. To reduce scatter in the values of  $T_2^*$  obtained by removing the contribution from the lifetime, the  $T_1$  values at each temperature were obtained from the linear fit to all of the  $T_1$  data.

Figure 3 displays the values of the pure dephasing time versus inverse temperature on semilog plot.<sup>14</sup> The solid line through the data is a fit to the form

$$\frac{1}{T_2^*} = a_1 T^\alpha + a_2 e^{-\Delta E/kT} \quad (3)$$

with  $\alpha = 1$  and  $\Delta E = 385$  cm<sup>-1</sup>. Note that there is no break in the temperature dependence at  $T_g = 169$  K (see inset). Also shown are dotted and dashed lines, in which  $\alpha$  is fixed at 0.7 and 1.3, respectively, and the other parameters are allowed to float. Within experimental error,  $\alpha = 1.0$  gives the best fit to the data, and the value of  $\alpha$  has only a very minor effect on the activation energy. By considering a variety of fits such as those displayed in Fig. 3, the best values for  $\alpha$  and  $\Delta E$  are  $\alpha = 1.0 \pm 0.1$  and  $\Delta E = 385 \pm 50$  cm<sup>-1</sup>.

The Rh(CO)<sub>2</sub>acac pure dephasing temperature dependence is different from that previously observed for the pure dephasing of the  $T_{1u}$  mode of W(CO)<sub>6</sub> in three glass forming solvents. Figure 4 shows  $1/(\pi T_2^*)$  for W(CO)<sub>6</sub> in DBP from 10 K to just above  $T_g$  on a log plot.<sup>9,10</sup> The straight line through the data yields a temperature dependence of  $T^2$  over the entire temperature range. Clearly the temperature dependence of the pure dephasing of the two compounds in the glass is fundamentally different even though the pure dephasing is for a CO asymmetric stretching mode of both molecules at ~2000 cm<sup>-1</sup> in the same solvent.

Figure 5 shows a reduced variable plot of the homogeneous dephasing of the  $T_{1u}$  mode of W(CO)<sub>6</sub> in three glassy solvents, DBP, 2MP, and 2-methyltetrahydrofuran (2MTHF).<sup>9</sup> The solid line through the data is  $T^2$ . Within

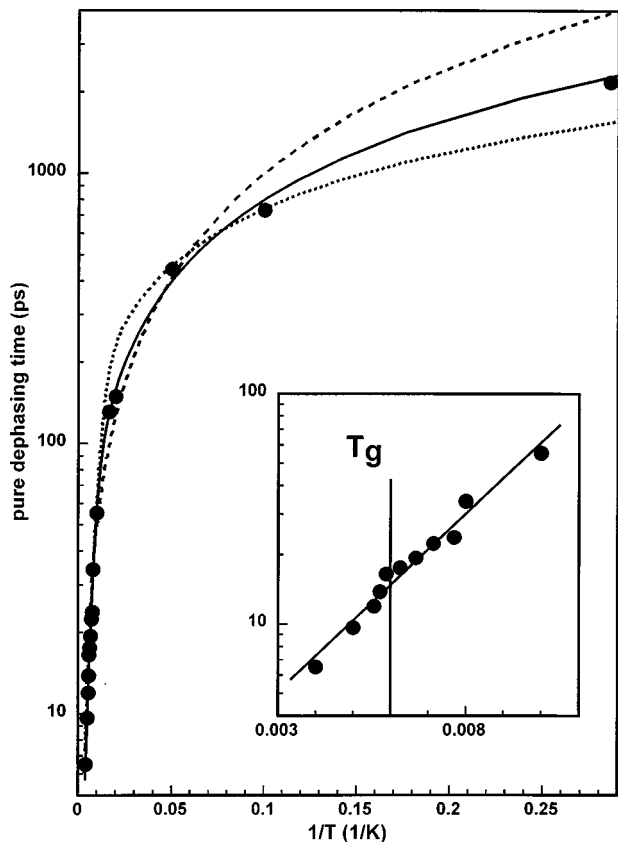


FIG. 3. Pure dephasing time of the asymmetric CO stretch mode of  $\text{Rh}(\text{CO})_2\text{acac}$  in DBP versus inverse temperature on a semi-log plot. The solid line through the data is a fit to Eq. (3), the sum of a power law and an exponentially activated process. Note that there is no break at the experimental  $T_g$ , 169 K. The inset is an expanded view at high temperatures showing that the process is activated. The best fit has the power law exponent,  $\alpha = 1.0$  and  $\Delta E = 385 \text{ cm}^{-1}$ . Dotted and dashed lines are with  $\alpha$  in Eq. (3) fixed at 0.7 and 1.3, respectively, and the other parameters of Eq. (3) are allowed to float.

experimental error, the homogeneous dephasing has a  $T^2$  temperature dependence in all three solvents in spite of the fact that the three solvents are quite different.

A full temperature dependence of the pure dephasing of  $\text{W}(\text{CO})_6$  is only available in the solvent 2MP.<sup>9,10</sup> The

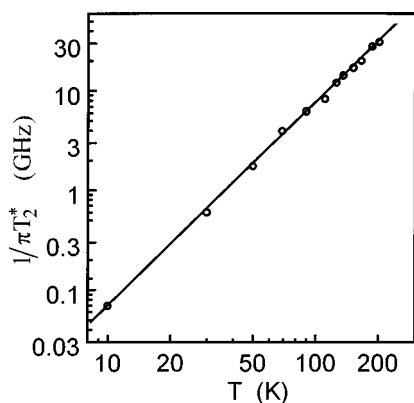


FIG. 4. Pure dephasing rate of  $\text{W}(\text{CO})_6$  in DBP versus temperature on a log plot. The straight line through the data is a fit which yields a  $T^2$  dependence.

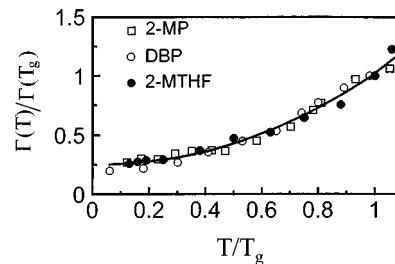


FIG. 5. Reduced variable plot of the homogeneous dephasing of  $\text{W}(\text{CO})_6$  in DBP, 2MP, and 2MTHF. The abscissa is the homogeneous line width divided by the homogeneous line width at  $T_g$ . The ordinate is  $T$  scaled by  $T_g$ . All data sets fall on the  $T^2$  line.

$\text{W}(\text{CO})_6$  in 2MP displays orientational relaxation because of a mechanism that depends on the degeneracy of the  $T_{1u}$  mode (see below). The temperature dependences of the orientational relaxation as well as  $T_2$  and  $T_1$  have been measured.<sup>10</sup> Using these, the temperature dependence of the pure dephasing was obtained and is displayed in Fig. 6 on a log plot. Below  $T_g$ , the temperature dependence is  $T^2$ , as discussed above. Above  $T_g$ , there is a dramatic break in the temperature dependence. The solid line through the data is a fit to Eq. (4),

$$\frac{1}{\pi T_2^*} = a_1 T^\alpha + a_2 \exp(-B/(T - T_0)), \quad (4)$$

where  $\alpha$  is  $2.0 \pm 0.1$ . The first term is the  $T^2$  temperature dependence observed in the low-temperature glass. The second term has the form of the VTF equation which is often used to describe the onset of dynamic processes near the  $T_g$ .<sup>24-26</sup> The VTF equation describes a process with a temperature-dependent activation energy that diverges at a

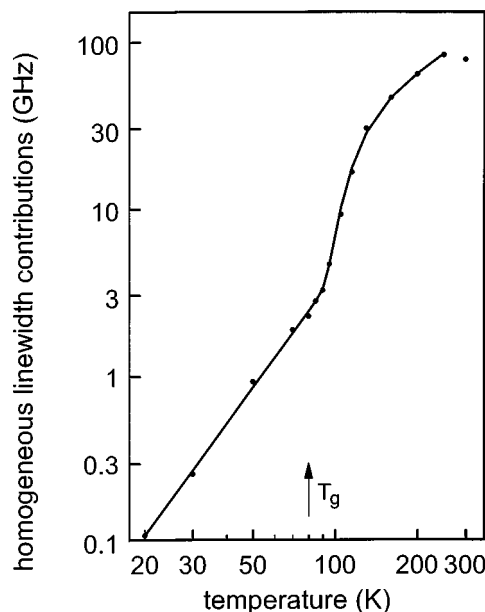


FIG. 6. Temperature dependence of the pure dephasing of the asymmetric CO stretch of  $\text{W}(\text{CO})_6$  in 2MP. The line through the pure dephasing data is a fit to Eq. (4).

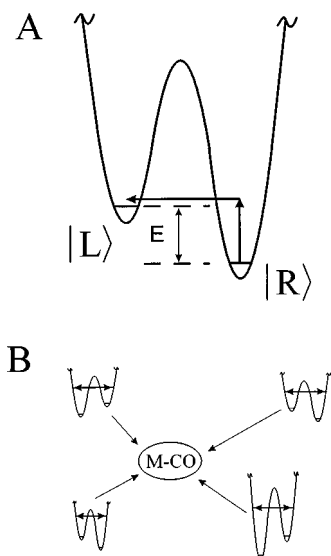


FIG. 7. (a) An illustration of a two-level system (TLS) making a transition from a lower energy local structure in the glass to a higher energy structure. A glass is modeled as having many TLS with a broad distribution of tunneling splittings,  $E$ . (b) A schematic of the CO oscillator coupled to a number of TLSs. The TLS transitions produce fluctuating forces at the oscillator causing pure dephasing.

temperature,  $T_0$ , below the nominal  $T_g$ .  $T_0$  can be linked thermodynamically to an “ideal”  $T_g$ .<sup>24</sup> This equation describes the temperature dependence of the viscosity of 2MP well, and gives  $T_0 = 59$  K.<sup>9</sup> The fit of Eq. (4) to the pure dephasing data describes the entire temperature dependence exceedingly well up to 250 K, but yields a reference temperature of  $T_0 = 80$  K. This reference temperature matches the laboratory  $T_g$ , not the ideal  $T_g$ . The onset of the dynamics that cause the rapid increase in homogeneous dephasing of  $\text{W}(\text{CO})_6$  in 2MP is apparently linked with the onset of structural processes near the laboratory  $T_g$ .

## IV. DEPHASING MECHANISMS

### A. Low-temperature pure dephasing of $\text{Rh}(\text{CO})_2\text{acac}$

Pure dephasing of the form  $T^\alpha$  where  $\alpha \approx 1$  has been seen repeatedly for homogeneous pure dephasing of electronic transitions of molecules in low-temperature glasses using photon echoes<sup>3,27,28</sup> and hole burning spectroscopy.<sup>1,29–31</sup> The electronic dephasing has been described using the two-level system (TLS) model of low-temperature glass dynamics<sup>3,29,32,33</sup> that was originally developed in the early 70s to explain the anomalous heat capacity of low-temperature glasses, which is approximately linear in  $T$ .<sup>34,35</sup> Even at low temperatures, glasses are continuously undergoing structural changes. The complex potential surface on which local structural dynamics occur is modeled as a collection of double wells. At low temperatures, only the lowest energy levels are involved, so these are referred to as TLS. Figure 7(a) is an illustration of a TLS.  $|L\rangle$  represents a particular local structure of the glass.  $|R\rangle$  represents a different local structure. Transitions can be made between  $|L\rangle$  and  $|R\rangle$  by phonon-assisted tunneling. At very low temperatures,

where the Debye  $T^3$  contribution to the heat capacity is small, the heat capacity is dominated by the uptake of energy in going from a lower energy structure to a higher energy structure, e.g., the transition  $|R\rangle \Rightarrow |L\rangle$  in Fig. 7(a). A glass is modeled as having many TLSs with a broad distribution of tunnel splittings,  $E$ . If the probability,  $P(E)$ , of having a splitting  $E$  is constant,  $P(E) = C$ , (all  $E$ 's are equally probable), then the heat capacity is  $T^1$ .

The description of electronic dephasing in low-temperature glasses is based on the TLS dynamics.<sup>3,29,32,33</sup> We propose that identical considerations can apply to the vibrational dephasing of  $\text{Rh}(\text{CO})_2\text{acac}$  in DBP at low temperature. Figure 7(b) illustrates the mechanism. A particular molecule is coupled to a number of TLS. For those TLS with  $E$  not too large ( $E \leq 2kT$ ), the TLS are constantly making transition between  $|L\rangle$  and  $|R\rangle$  with a rate determined by  $E$  and the tunneling parameter.<sup>2</sup> The structural changes between  $|L\rangle$  and  $|R\rangle$  produce fluctuating strains or fluctuating electric dipoles. The fluctuating strains or dipoles produce fluctuating forces on the CO oscillator. Thus, the vibrational pure dephasing can be caused by TLS dynamics. It has been demonstrated theoretically using the uncorrelated sudden jump model that for  $P(E) = CE^\mu$ , the temperature dependence of the pure dephasing is  $T^{1+\mu}$ .<sup>3,36–38</sup> Therefore, for the flat distribution,  $\mu = 0$ , the pure dephasing temperature dependence is  $T^1$ .  $T^1$  and somewhat steeper temperature dependences, e.g.,  $T^{1.3}$ , have been observed in electronic dephasing experiments in low-temperature glasses.<sup>1,3,27,36</sup> Recent theoretical work that has examined the problem in more detail suggests that even the apparent super linear temperature dependences may arise from an energy distribution  $P(E) = C$ .<sup>39</sup> Other theoretical work has investigated the influence of coupled TLS.<sup>40</sup> Regardless of the theoretical approach, the qualitative results are the same. Coupling of a transition to a distribution of tunneling TLS can produce pure dephasing which is essentially  $T^1$ .

### B. High-temperature pure dephasing of $\text{Rh}(\text{CO})_2\text{acac}$

Above  $\sim 20$  K, the  $T^1$  vibrational pure dephasing is dominated by the exponentially activated process. Electronic dephasing experiments have also shown power law temperature dependences that go over to activated processes at higher temperatures.<sup>41–43</sup> However, in the electronic experiments, power law behavior is observed only to a few degrees K because typical activation energies for electronic dephasing are  $15\text{--}30$   $\text{cm}^{-1}$ .<sup>42,43</sup> Therefore, the activated process begins to dominate the power law pure dephasing at lower temperatures than is observed for the CO vibrational dephasing of  $\text{Rh}(\text{CO})_2\text{acac}$ . The low activation energy for electronic dephasing in glasses has been shown to arise from coupling of the electronic transition to low-frequency modes of the glass.<sup>42,43</sup> In the vibrational dephasing experiments, the  $\Delta E \cong 400$   $\text{cm}^{-1}$ . Thus, the power law component of the temperature dependence is not masked until higher temperatures.

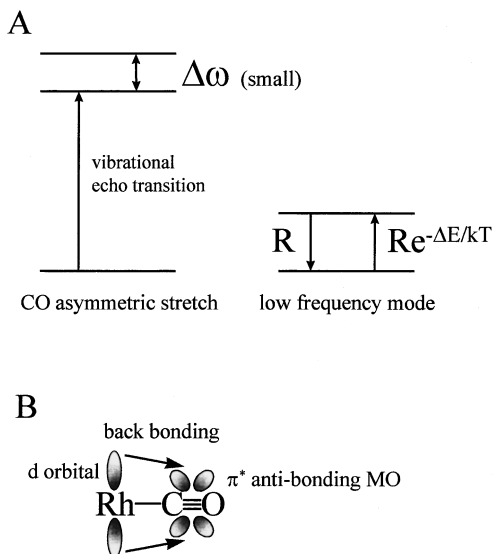


FIG. 8. (a) Proposed dephasing mechanism of the asymmetric CO stretching mode of  $\text{Rh}(\text{CO})_2\text{acac}$  at high temperature. Thermal activation of a low-frequency mode causes a small change in the transition frequency,  $\Delta\omega$ , of the high-frequency mode. During the time when the low-frequency mode is excited, the high-frequency mode develops a phase error. (b) Electron donation from the  $d_\pi$  orbital of the Rh atom to the CO  $\pi^*$  antibonding molecular orbital of CO. Thermal excitation of the Rh–C stretch will lengthen the bond which decreases the magnitude of backbonding, producing a shift to higher energy of the CO transition.

In the  $\text{Rh}(\text{CO})_2\text{acac}$  system, the temperature dependence of the pure dephasing changes rapidly above  $\sim 20$  K. By 100 K, the temperature dependence is well described by the activated process alone (see inset in Fig. 3). There is no break in the pure dephasing data as the sample passes through  $T_g$ . The activation energy,  $\Delta E = \sim 400 \text{ cm}^{-1}$ , is well above the typical cutoff for phonon modes of organic solids.<sup>44</sup> Furthermore, the far-IR absorption spectra of neat DBP shows no strong transitions in the region around  $400 \text{ cm}^{-1}$ , indicating that there is no specific mode of the solvent that might couple strongly to the CO mode. These facts suggest that the high temperature Arrhenius dephasing process is not caused by a motion associated with the glass/liquid solvent, but rather that the dephasing arises from coupling of the CO mode to an internal mode of  $\text{Rh}(\text{CO})_2\text{acac}$ .

The proposed mechanism is illustrated in Fig. 8(a). Thermal excitation of a low-frequency mode causes the CO stretching mode transition frequency to shift a small amount,  $\Delta\omega$ . The lifetime of the low-frequency mode is  $\tau = 1/R$ . During the time period in which the low-frequency mode is excited, the initially prepared CO superposition state precesses at a higher frequency. Thus, a phase error develops. For a small  $\Delta\omega$  and a short  $\tau$ , the phase error is on the order of  $\tau\Delta\omega < 1$ . This is the slow or intermediate exchange limit.<sup>45,46</sup> Repeated excitation and relaxation of the low-frequency mode will produce homogeneous dephasing.<sup>45,46</sup>

Over a temperature range in which the energy of the low-frequency transition,  $\Delta E$ , is large compared to  $kT$ , the rate of excitation of the low-frequency mode increases exponentially with temperature, i.e., the rate of excitation is

$\text{Re}^{-\Delta E/kT}$ . Over this same temperature range, the downward rate will be temperature independent or have a weak temperature dependence. From the fit,  $\Delta E \cong 400 \text{ cm}^{-1}$  and the highest experimental temperature corresponds to  $\sim 170 \text{ cm}^{-1}$ , so this condition is met. This system is in the weak coupling limit, i.e., the change in the CO frequency,  $\Delta\omega$ , with excitation of the low-frequency mode is small compared to the CO frequency. In addition,  $\hbar|\Delta\omega|/kT \ll 1$ . For these conditions, the pure dephasing contribution to the linewidth from repeated excitation and relaxation of the low-frequency mode is<sup>45</sup>

$$\frac{1}{\pi T_2^*} = \frac{1}{\tau} \left[ \frac{(\Delta\omega\tau)^2}{1 + (\Delta\omega\tau)^2} \right] e^{-\Delta E/kT}. \quad (5)$$

Equation (5) shows that this contribution to the homogeneous linewidth is exponentially activated. The right-hand side of Eq. (5) is consistent with Eq. (3), which was used to fit the data. The factor multiplying the exponential is the constant  $a_2$  in Eq. (3). This term dominates the temperature dependence at high temperature.

For the proposed mechanism to account for the observed high temperature pure dephasing, a mode of  $\sim 400 \text{ cm}^{-1}$  must couple nonnegligibly to the asymmetric CO stretch so that  $\Delta\omega$  is significant. The Rh–C asymmetric stretching mode has a transition energy of  $405 \text{ cm}^{-1}$ .<sup>47</sup> The closest other modes of  $\text{Rh}(\text{CO})_2\text{acac}$  are outside of the error bars on the activation energy.<sup>47</sup> There is a reasonable explanation why the Rh–C stretch couples significantly to the CO mode, but modes of lower frequency, which would become populated at lower temperature, do not. The explanation is illustrated in Fig. 8(b). The  $\text{Rh}(\text{CO})_2\text{acac}$  has significant back donation of electron density from the Rh  $d_\pi$  to the CO  $p_{\pi^+}$  antibonding orbital (back bonding) that weakens the CO bond and red shifts the transition energy about  $100$  to  $\sim 2045 \text{ cm}^{-1}$ . (The splitting of the symmetric and asymmetric linear combination of the 2 CO stretches further shifts the asymmetric mode to the observed value of  $2010 \text{ cm}^{-1}$ .) Thus, back bonding plays a significant role in determining the transition frequency. It is well known that in metal-carbonyl compounds, the CO frequency is very sensitive to changes in back bonding.<sup>48</sup> Also, a combination of isotope substitution spectroscopic experiments and calculations show that for metal-carbonyls, there is substantial coupling between the M–C stretch and the C–O stretch.<sup>49</sup> When the Rh–C mode is thermally excited from the  $v=0$  state to the  $v=1$  state, the average bond length will increase. The increase in the sigma bond length will decrease the Rh  $d_\pi$ –CO  $p_{\pi^+}$  orbital overlap, and, therefore, decrease the magnitude of the back bonding. Thus, excitation of the Rh–C mode causes a blue shift of the CO stretching frequency by decreasing the back bonding.<sup>14</sup>

Although data is not available for  $\text{Rh}(\text{CO})_2\text{acac}$ , IR absorption measurements on transition metal hexacarbonyls support this mechanism.<sup>49</sup> For the equivalent mode of  $\text{M}(\text{CO})_6$  ( $\text{M}=\text{Mo}, \text{Cr}$ ), the combination absorption band of the M–C asymmetric stretch and the CO asymmetric stretch is  $\sim 20 \text{ cm}^{-1}$  higher in energy than the sum of the two fun-

damental energies.<sup>49</sup> Thus,  $\Delta\omega \approx 20 \text{ cm}^{-1}$ . The change in back bonding upon excitation of the Rh–C mode provides a direct mechanism for coupling excitation of the Rh–C stretch to the CO stretch transition frequency. Other low-frequency modes, such as a methyl rocking mode of the acac ligand, will not have this type of direct coupling, and, therefore, will not cause dephasing even though they may be thermally populated.

If the proposed mechanism is valid, it should be possible to reproduce the constant  $a_2$  in Eq. (3) using Eq. (5) with reasonable values of the other parameters:

$$a_2 = \frac{1}{\pi\tau} \left[ \frac{(\Delta\omega\tau)^2}{1 + (\Delta\omega\tau)^2} \right]. \quad (6)$$

The value of  $a_2$  is obtained from the data in Fig. 3;  $a_2 = 1.2 \times 10^{12} \text{ Hz}$ . As discussed above, based on compounds similar to  $\text{Rh}(\text{CO})_2\text{acac}$ ,  $\Delta\omega \approx 20 \text{ cm}^{-1}$ . Using the values for  $a_2$  and  $\Delta\omega$  yields a value of  $\tau \approx 0.75 \text{ ps}$  is obtained for the vibrational lifetime of the  $405 \text{ cm}^{-1}$  Rh–C stretch. Direct measurements of the lifetime of this mode or of any low frequency vibrations have not been made. However, 0.75 ps is a plausible number. The Rh–C mode can relax via a cubic anharmonic process involving the annihilation of the original Rh–C excitation and the creation of two lower frequency modes.<sup>47</sup> The  $\text{Rh}(\text{CO})_2\text{acac}$  has several internal lower frequency modes.<sup>47</sup> One possible relaxation pathway is to create one internal mode, e.g.,  $300 \text{ cm}^{-1}$ , and create a mode of the solvent continuum, assuring conservation of energy. Another possible pathway is relaxation into two modes of the solvent continuum. For a nonhydrogen bonding solvent such as DBP, the continuum of translational and orientational modes (instantaneous normal modes<sup>50,51</sup>) will extend to several hundred  $\text{cm}^{-1}$ .<sup>52</sup> For either possibility, the low-order cubic anharmonic processes available for the relaxation and the high density of states provided by the solvent continuum will cause rapid relaxation of the Rh–C vibration. In the future, it may be possible to perform a far IR pump-probe experiment to make a direct measurement of the Rh–C lifetime.

### C. Dephasing of $\text{W}(\text{CO})_6$

As can be seen from a comparison of Figs. 3, 4, and 6, the temperature-dependent pure dephasing of  $\text{Rh}(\text{CO})_2\text{acac}$  is fundamentally different from that of  $\text{W}(\text{CO})_6$  at all temperatures even though an asymmetric CO stretch at  $\sim 2000 \text{ cm}^{-1}$  was studied in both molecules. It is proposed that the  $\text{W}(\text{CO})_6$  pure dephasing is different because of the high symmetry of the  $T_{1u}$  asymmetric CO stretching mode, which makes it triply degenerate in the gas phase,<sup>49</sup> while the  $\text{Rh}(\text{CO})_2\text{acac}$  mode is not degenerate. The  $\text{W}(\text{CO})_6 T_{1u}$  mode consists of all six CO's moving in concert, one pair along the molecular  $x$  axis, one pair along  $y$ , and one pair along  $z$ . In a liquid or glass, the local solvent structure is anisotropic. In general, there will be different solute/solvent interactions (forces exerted on the oscillator) along  $x$ ,  $y$ , and  $z$ . These interactions will break the triple degeneracy, yielding three

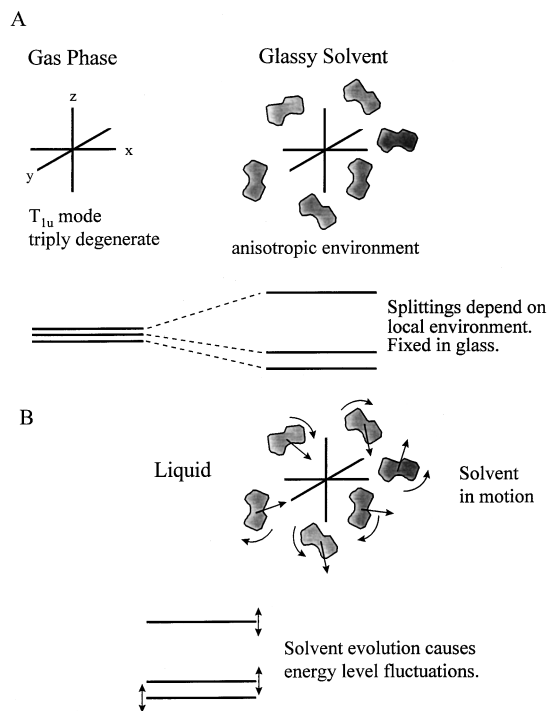


FIG. 9. (a) In the gas phase, the  $T_{1u}$  mode of  $\text{W}(\text{CO})_6$  is triply degenerate. In a condensed phase, such as a liquid or glass, the anisotropic environment breaks the degeneracy, producing three levels with small energy splittings. (b) Solvent molecular motions in the liquid state produce a local, time-dependent anisotropic structure. Fluctuations in local structure couple to the three levels, causing energy level fluctuations and pure dephasing.

modes with small energy splittings. This model is illustrated in Fig. 9(a). There will be a range of such splittings reflecting the range of local solvent structures.

In a glass, the local solvent structure about  $\text{W}(\text{CO})_6$  is essentially fixed on the time scale of the pure dephasing. The  $T^2$  temperature dependence in the three glassy solvents studied suggests a two phonon process in the high-temperature limit, i.e.,  $kT > \hbar\omega_p$ , where  $\omega_p$  is a typical phonon frequency involved in the two phonon process. Two phonon elastic scattering that causes fluctuations in the anisotropic local solvent structure surrounding  $\text{W}(\text{CO})_6$  will induce fluctuations of the level splittings and can cause pure dephasing.

A second mechanism that would result in a  $T^2$  temperature dependence is two phonon scattering from one level to another. This mechanism is referred to as inelastic two phonon scattering. This second possibility can be ruled out. The nondegenerate levels will be approximately the molecular  $x$ ,  $y$ , and  $z$  basis modes of the triply degenerate state, although there may be some mixing caused by the anisotropic nature of the solvent perturbation. Scattering among the levels would result in orientational relaxation since it will take the oscillating dipole from, for example,  $x$  to  $y$  or  $z$ . In both the glass and liquid states of the solvent, the contribution of orientational relaxation to the total homogeneous line width has been analyzed, and it is small compared the other contributions.<sup>9</sup> If two phonon inelastic scattering among the three nondegenerate levels were responsible for the pure

dephasing, it would occur at the same rate as the orientational relaxation.

In the previous studies, orientational relaxation, which was shown not to depend on physical rotation of the molecule, was ascribed to the triply degenerate nature of the  $T_{1u}$  state.<sup>9,10</sup> However, it was implicitly assumed that the state was actually degenerate, and that the radiation field would excite some particular coherent superposition of the  $x$ ,  $y$ , and  $z$  basis states.<sup>9</sup> Because the degeneracy is broken by the anisotropic environment, a single state will be excited. The probability of exciting  $x$ ,  $y$ , or  $z$  will depend on the projection of the excitation  $E$ -field onto the molecular  $x$ ,  $y$ , and  $z$  axes. Then, the overall proposal is that orientational relaxation is caused by two-phonon inelastic scattering among the three nondegenerate states, and, in the glass, pure dephasing is caused by two-phonon elastic-scattering-induced fluctuations of the  $x$ ,  $y$ , and  $z$  levels. Because the  $T_{1u}$  mode is initially degenerate, any anisotropic perturbation will break the degeneracy. The resulting splittings are very sensitive to even small phonon-induced fluctuations of the local solvent environment. This is not a mechanism that is available to  $\text{Rh}(\text{CO})_2\text{acac}$ . Apparently, the two-phonon elastic scattering mechanism available to  $\text{W}(\text{CO})_6$  dominates the mechanisms responsible for pure dephasing of  $\text{Rh}(\text{CO})_2\text{acac}$  in the glass and liquid states.

The temperature dependence of the total homogeneous line widths of  $\text{W}(\text{CO})_6$  changes abruptly above  $T_g$  in the three solvents, DBP, 2MTHF, and 2MP.<sup>9,10</sup> In DBP and 2MTHF, there is evidence of motional narrowing.<sup>9,10</sup> The pure vibrational dephasing above  $T_g$  in 2MP has the very steep VTF temperature dependence (see Fig. 6). In the liquid, the solvent structure surrounding  $\text{W}(\text{CO})_6$  is no longer static on the homogeneous time scale [see Fig. 9(b)]. Translation and rotational motions of the solvent will produce fluctuating forces that do not occur below  $T_g$ . Thus, there is a change from a two-phonon elastic scattering mechanism with essentially fixed solvent structure below  $T_g$  to a mechanism that involves the evolution of the local anisotropic solvent structure above  $T_g$ .

The evolution of the local solvent structure will cause the splittings of the three closely spaced levels to evolve in time, inducing pure dephasing [see Fig. 9(b)]. Thus, the triply degenerate nature of the  $\text{W}(\text{CO})_6$   $T_{1u}$  mode is also intimately involved in the pure dephasing in the liquid, but the nature of the solvent dynamics changes above  $T_g$ , causing the abrupt change in the temperature dependence. In the proposed mechanism, the pure dephasing of  $\text{W}(\text{CO})_6$  in liquid 2MP is caused by the very-high-frequency solvent motions that are ultimately responsible for longer time scale processes such as translational and rotational diffusion and dielectric relaxation. The observed VTF temperature dependence would seem to be consistent with this dephasing mechanism.

## V. CONCLUDING REMARKS

Vibrational echo experiments have made it possible to perform a detailed examination of the dynamics of inter- and

intramolecular interactions that give rise to the homogeneous line widths and pure dephasing of the asymmetric stretching modes of  $\text{Rh}(\text{CO})_2\text{acac}$  and  $\text{W}(\text{CO})_6$  in liquid and glassy solvents. Even when  $\text{Rh}(\text{CO})_2\text{acac}$  and  $\text{W}(\text{CO})_6$  are in the same solvent, the functional forms of their temperature-dependent pure dephasing are very different. At low temperature (3.5 K to  $\sim 20$  K),  $\text{Rh}(\text{CO})_2\text{acac}$  pure dephasing goes as  $T^1$ . This is interpreted as the result of coupling of the vibrational mode to the dynamical two-level systems of the glassy DBP solvent. Above  $\sim 20$  K, the pure dephasing becomes exponentially activated with an activation energy of  $\sim 400$   $\text{cm}^{-1}$ . There is no change in the functional form of the temperature dependence in passing from the glass to the liquid. These results suggest that the activated process arises from coupling of the high-frequency CO stretch to the internal  $405$   $\text{cm}^{-1}$  Rh–C asymmetric stretching mode. Excitation of the Rh–C stretch produces changes in the back donation of electron density from the metal  $d_\pi$  orbitals to the CO  $\pi^*$  anti-bonding orbital, shifting the CO stretching transition frequency and causing dephasing.

The pure dephasing of  $\text{W}(\text{CO})_6$  has a  $T^2$  temperature dependence in DBP, 2MP, and 2MTHF glasses. In all three solvents, there is an abrupt change in the functional form of the temperature dependence in going from the glass to the liquid. In liquid 2MP, the pure dephasing has a VTF temperature dependence. The major differences in the temperature-dependent pure dephasing of the asymmetric stretching modes of  $\text{Rh}(\text{CO})_2\text{acac}$  and  $\text{W}(\text{CO})_6$  are attributed to the difference in the degeneracy of the modes. The  $\text{Rh}(\text{CO})_2\text{acac}$  mode is nondegenerate while the  $\text{W}(\text{CO})_6$  mode is triply degenerate in the gas phase. When  $\text{W}(\text{CO})_6$  is placed in a glass or liquid solvent, the local anisotropic solvent structure breaks the degeneracy, yielding three modes with small energy splittings. The results indicate that these splittings are very sensitive to local fluctuations in the solvent, giving rise to dephasing mechanisms that are not available to  $\text{Rh}(\text{CO})_2\text{acac}$ . The abrupt change in the temperature dependence of the  $\text{W}(\text{CO})_6$  vibrational pure dephasing above  $T_g$  occurs because the nature of the local solvent structural fluctuations change in going from a glass to a liquid.

It is interesting and useful to note that the two molecules studied provide probes of different aspects of solvent dynamics. At low temperature, the vibrational pure dephasing of  $\text{Rh}(\text{CO})_2\text{acac}$  is sensitive to the glass's structural evolution produced by two level system dynamics, while that of  $\text{W}(\text{CO})_6$  is not. However, above  $T_g$ , the broken degeneracy of the  $T_{1u}$  mode of  $\text{W}(\text{CO})_6$  causes its vibrational pure dephasing to be sensitive to the dynamics of the supercooled liquid, while the nondegenerate mode of  $\text{Rh}(\text{CO})_2\text{acac}$  is not.

The observed differences between the vibrational pure dephasing of the asymmetric stretching modes of  $\text{Rh}(\text{CO})_2\text{acac}$  and  $\text{W}(\text{CO})_6$  have been attributed to the difference in the mode degeneracy. Future vibrational echo experiments on other metal carbonyls and vibrations of other classes of molecules will continue to explore the nature of vibrational pure dephasing in liquids, glasses, and proteins.<sup>53,54</sup>

## ACKNOWLEDGMENTS

We would like to thank Professor James Skinner, Department of Chemistry, University of Wisconsin at Madison, for very useful conversations pertaining to this work. We would also like to thank Dr. C. W. Rella, Dr. A. S. Kwok, and Dr. C. Ferrante for their assistance in performing some of the experiments, and Professors Alan Schwettman and Todd Smith, Physics Department, Stanford University, and their research groups at the Stanford FEL Center whose efforts made these experiments possible. This research was supported by the National Science Foundation, Division of Materials Research (DMR-9610326), and the Office of Naval Research (N00014-94-1-1024, N00014-92-J-1227-P00006, and N00014-97-1-0899).

- <sup>1</sup>H. P. H. Thijssen, A. I. M. Dicker, and S. Völker, *Chem. Phys. Lett.* **92**, 7 (1982).
- <sup>2</sup>D. Harrer, *Photochemical Hole-Burning in Electronic Transitions* (Springer-Verlag, Berlin, 1988).
- <sup>3</sup>L. R. Narasimhan, K. A. Littau, D. W. Pack, Y. S. Bai, A. Elschner, and M. D. Fayer, *Chem. Rev.* **90**, 439 (1990).
- <sup>4</sup>S. Fei, G. S. Yu, H. W. Li, and H. L. Strauss, *J. Chem. Phys.* **104**, 6398 (1996).
- <sup>5</sup>A. Tokmakoff, R. S. Urdahl, D. Zimdars, R. S. Francis, A. S. Kwok, and M. D. Fayer, *J. Chem. Phys.* **102**, 3919 (1994).
- <sup>6</sup>E. L. Hahn, *Phys. Rev.* **80**, 580 (1950).
- <sup>7</sup>N. A. Kurnit, I. D. Abella, and S. R. Hartmann, *Phys. Rev. Lett.* **13**, 567 (1964).
- <sup>8</sup>I. D. Abella, N. A. Kurnit, and S. R. Hartmann, *Phys. Rev. Lett.* **14**, 391 (1966).
- <sup>9</sup>A. Tokmakoff and M. D. Fayer, *J. Chem. Phys.* **102**, 2810 (1995).
- <sup>10</sup>A. Tokmakoff, D. Zimdars, R. S. Urdahl, R. S. Francis, A. S. Kwok, and M. D. Fayer, *J. Phys. Chem.* **99**, 13 310 (1995).
- <sup>11</sup>A. Tokmakoff and M. D. Fayer, *Acc. Chem. Res.* **28**, 437 (1995).
- <sup>12</sup>K. S. Schweizer and D. Chandler, *J. Chem. Phys.* **76**, 2240 (1982).
- <sup>13</sup>D. W. Oxtoby, *Annu. Rev. Phys. Chem.* **32**, 77 (1981).
- <sup>14</sup>K. D. Rector, A. S. Kwok, C. Ferrante, R. S. Francis, and M. D. Fayer, *Chem. Phys. Lett.* **276**, 217 (1997).
- <sup>15</sup>D. Zimdars, A. Tokmakoff, S. Chen, S. R. Greenfield, and M. D. Fayer, *Phys. Rev. Lett.* **70**, 2718 (1993).
- <sup>16</sup>T. C. Farrar and D. E. Becker, *Pulse and Fourier Transform NMR* (Academic, Press, New York, 1971).
- <sup>17</sup>J. L. Skinner, H. C. Anderson, and M. D. Fayer, *J. Chem. Phys.* **75**, 3195 (1981).
- <sup>18</sup>R. G. Gordon, *J. Chem. Phys.* **43**, 1307 (1965).
- <sup>19</sup>R. G. Gordon, *Adv. Magn. Reson.* **3**, 1 (1968).
- <sup>20</sup>B. J. Berne, *Physical Chemistry: An Advanced Treatise* (Academic, New York, 1971).
- <sup>21</sup>D. A. Zimdars, Graduate thesis, Stanford University, 1996.
- <sup>22</sup>K. D. Rector, A. S. Kwok, C. Ferrante, A. Tokmakoff, C. W. Rella, and M. D. Fayer, *J. Chem. Phys.* **106**, 10027 (1997).
- <sup>23</sup>A. Tokmakoff, A. S. Kwok, R. S. Urdahl, R. S. Francis, and M. D. Fayer, *Chem. Phys. Lett.* **234**, 289 (1995).
- <sup>24</sup>C. A. Angell, *J. Phys. Chem. Solids Suppl.* **49**, 863 (1988).
- <sup>25</sup>C. A. Angell, *J. Phys. Chem.* **86**, 3845 (1982).
- <sup>26</sup>G. H. Fredrickson, *Annu. Rev. Phys. Chem.* **39**, 149 (1988).
- <sup>27</sup>L. W. Molenkamp and D. A. Wiersma, *J. Chem. Phys.* **83**, 1 (1985).
- <sup>28</sup>Y. G. Vainer, R. I. Personov, S. Zilker, and D. Haarer, in *Fifth International Meeting on Hole Burning and Related Spectroscopies: Science and Applications*, edited by G. J. Small (Gordon and Breach, Brainerd, MN, 1996), Vol. 291, pp. 51.
- <sup>29</sup>H. W. H. Lee, A. L. Huston, M. Gehrtz, and W. E. Moerner, *Chem. Phys. Lett.* **114**, 491 (1985).
- <sup>30</sup>J. M. Hayes, R. P. Stout, and G. J. Small, *J. Chem. Phys.* **74**, 4266 (1981).
- <sup>31</sup>R. M. Macfárlane and R. M. Shelby, *Opt. Commun.* **45**, 46 (1983).
- <sup>32</sup>R. M. Macfárlane and R. Shelby, *J. Lumin.* **36**, 179 (1987).
- <sup>33</sup>J. Friedrich, H. Wolfrum, and D. Haarer, *J. Chem. Phys.* **77**, 2309 (1982).
- <sup>34</sup>W. A. Phillips, *J. Low Temp. Phys.* **7**, 351 (1972).
- <sup>35</sup>P. W. Anderson, B. I. Halperin, and C. M. Varma, *Philos. Mag.* **25**, 1 (1972).
- <sup>36</sup>J. M. Hayes, R. Jankowiak, and G. J. Small, in *Persistent Spectral Hole Burning: Science and Applications*, edited by W. E. Moerner (Springer-Verlag, Berlin, 1988), Vol. 44, pp. 153.
- <sup>37</sup>D. L. Huber, *J. Non-Cryst. Solids* **51**, 241 (1982).
- <sup>38</sup>D. L. Huber, M. M. Broer, and B. Golding, *Phys. Rev. Lett.* **52**, 2281 (1984).
- <sup>39</sup>E. Geva and J. L. Skinner, *J. Chem. Phys.* **107**, 7630 (1997).
- <sup>40</sup>K. Kassner and R. Silbey, *J. Phys. C* **1**, 4599 (1989).
- <sup>41</sup>P. M. Selzer, D. L. Huber, D. S. Hamilton, W. M. Yen, and M. J. Weber, *Phys. Rev. Lett.* **36**, 813 (1976).
- <sup>42</sup>A. Elschner, L. R. Narasimhan, and M. D. Fayer, *Chem. Phys. Lett.* **171**, 19 (1990).
- <sup>43</sup>S. R. Greenfield, Y. S. Bai, and M. D. Fayer, *Chem. Phys. Lett.* **170**, 133 (1990).
- <sup>44</sup>A. I. Kitaigorodsky, *Molecular Crystals and Molecules* (Academic, New York, 1973).
- <sup>45</sup>D. Hsu and J. L. Skinner, *J. Chem. Phys.* **83**, 2097 (1985).
- <sup>46</sup>R. M. Shelby, C. B. Harris, and P. A. Cornelius, *J. Chem. Phys.* **70**, 34 (1978).
- <sup>47</sup>D. M. Adams and W. R. Trumble, *J. C. S. Dalton*, 690 (1974).
- <sup>48</sup>D. M. Adams, *Metal-Ligand and Related Vibrations* (St. Martin's, New York, 1968).
- <sup>49</sup>L. H. Jones, R. S. McDowell, and M. Goldblatt, *Inorg. Chem.* **8**, 2349 (1969).
- <sup>50</sup>R. M. Stratt, *Acc. Chem. Res.* **28**, 201 (1995).
- <sup>51</sup>T. Keyes, *J. Phys. Chem. A* **101**, 2921 (1997).
- <sup>52</sup>Y. J. Chang and E. W. Castner, Jr., *J. Phys. Chem. A* **100**, 3330 (1996).
- <sup>53</sup>C. W. Rella, K. D. Rector, A. S. Kwok, J. R. Hill, H. A. Schwettman, D. D. Dlott, and M. D. Fayer, *J. Phys. Chem.* **100**, 15 620 (1996).
- <sup>54</sup>K. D. Rector, C. W. Rella, A. S. Kwok, J. R. Hill, S. G. Sligar, E. Y. P. Chien, D. D. Dlott, and M. D. Fayer, *J. Phys. Chem. B* **101**, 1468 (1997).